Chemotherapeutic agents circumvent emergence of dasatinib-resistant BCR-ABL kinase mutations in a precise mouse model of Philadelphia chromosome–positive acute lymphoblastic leukemia

Nidal Boulos,[1] Heather L. Mulder,[1] Christopher R. Calabrese,[2] Jeffrey B. Morrison,[1] Jerold E. Rehg,[3] Mary V. Relling,[4] Charles J. Sherr,[5,6] and Richard T. Williams[1]

[1]Department of Oncology, [2]Animal Imaging Center, Departments of [3]Pathology, [4]Pharmaceutical Sciences, and [5]Genetics and Tumor Cell Biology, and [6]Howard Hughes Medical Institute, St Jude Children's Research Hospital, Memphis, TN

The introduction of cultured p185$^{BCR-ABL}$–expressing (p185$^+$) *Arf*$^{-/-}$ pre-B cells into healthy syngeneic mice induces aggressive acute lymphoblastic leukemia (ALL) that genetically and phenotypically mimics the human disease. We adapted this high-throughput Philadelphia chromosome–positive (Ph$^+$) ALL animal model for in vivo luminescent imaging to investigate disease progression, targeted therapeutic response, and ALL relapse in living mice. Mice bearing high leukemic burdens (simulating human Ph$^+$ ALL at diagnosis) entered remission on maximally intensive, twice-daily dasatinib therapy, but invariably relapsed with disseminated and/or central nervous system disease. Although relapse was frequently accompanied by the eventual appearance of leukemic clones harboring BCR-ABL kinase domain (KD) mutations that confer drug resistance, their clonal emergence required prolonged dasatinib exposure. KD P-loop mutations predominated in mice receiving less intensive therapy, whereas high-dose treatment selected for T315I "gatekeeper" mutations resistant to all 3 Food and Drug Administration–approved BCR-ABL kinase inhibitors. The addition of dexamethasone and/or L-asparaginase to reduced-intensity dasatinib therapy improved long-term survival of the majority of mice that received all 3 drugs. Although non–tumor-cell–autonomous mechanisms can prevent full eradication of dasatinib-refractory ALL in this clinically relevant model, the emergence of resistance to BCR-ABL kinase inhibitors can be effectively circumvented by the addition of "conventional" chemotherapeutic agents with alternate antileukemic mechanisms of action. (*Blood*. 2011;117(13):3585-3595)

Introduction

The Philadelphia chromosome (Ph), a balanced translocation between chromosomes 9 and 22, initiates both chronic myelogenous leukemia (CML) and a subset of Ph$^+$ acute lymphoblastic leukemias (ALLs) and directs expression of the BCR-ABL fusion protein, a potently oncogenic, constitutively active tyrosine kinase.[1] In CML, the p210$^{BCR-ABL}$ isoform is expressed in hematopoietic stem cells and in both myeloid and lymphoid progeny, whereas in Ph$^+$ ALL, expression of either of 2 alternative p185$^{BCR-ABL}$ or p210$^{BCR-ABL}$ oncogenic isoforms is restricted to the B-cell lineage.

The chronic phase of CML, which presents as an abnormal expansion of relatively mature myeloid cells, accelerates without treatment to lethal blast crisis characterized by the rapid proliferation and expansion of immature myeloid or lymphoid cells in hematopoietic tissues. Ph$^+$ ALL resembles the aggressive lymphoid blast crisis of CML, but arises without a preceding indolent phase. During the chronic phase, affected CML cells do not typically harbor recurring regions of genomic amplification or loss, implying that BCR-ABL expression is sufficient to initiate disease.[2,3] In contrast, the malignant cells recovered from Ph$^+$ ALL and CML patients in lymphoid blast crisis also exhibit frequent deletions of the *IKZF1* (*IKAROS*) and *CDKN2A/B* (*INK4A/B-ARF*) tumor-suppressor genes (85% and 64% deletion frequencies, respectively, in untreated Ph$^+$ ALL cases). Inactivation of the latter genes affects the differentiation and self-renewal of immature pre-B cells and likely contributes to the highly aggressive nature of Ph$^+$ ALL.[2-4]

Targeted, continuous monotherapy of CML with imatinib, the first-generation US Food and Drug Administration (FDA)–approved BCR-ABL tyrosine kinase inhibitor (TKI), maintains most chronic-phase patients in remission.[1,5] However, because of the persistence of residual cells expressing BCR-ABL, imatinib discontinuation is often promptly followed by clinical relapse.[6] In addition, a small percentage of these patients relapse despite continuous imatinib exposure. Drug resistance is frequently associated with the development of mutations in the BCR-ABL kinase domain (KD) that impair drug binding.[7] Alternatively, altered dynamics of drug import and efflux or parallel signaling pathways that sustain leukemic-cell survival can contribute to drug resistance.[8] Second-generation BCR-ABL kinase inhibitors, including nilotinib and dasatinib, which are capable of inhibiting commonly encountered drug-resistant KD mutant alleles, were FDA-approved for use in patients with imatinib-resistant or intolerant CML and for Ph$^+$ ALL.[9-11] The T315I KD "gatekeeper" mutation renders the BCR-ABL kinase refractory to all 3 approved TKIs, which is consistent with clinical observations that this allele emerges most frequently when CML

Submitted August 11, 2010; accepted January 5, 2011. Prepublished online as *Blood* First Edition paper, January 24, 2011; DOI 10.1182/blood-2010-08-301267.

The online version of this article contains a data supplement.

The publication costs of this article were defrayed in part by page charge payment. Therefore, and solely to indicate this fact, this article is hereby marked "advertisement" in accordance with 18 USC section 1734.

patients are treated with broader-spectrum, more potent second-generation inhibitors.[12]

Although BCR-ABL TKIs induce significant hematologic and molecular responses when delivered as monotherapy, remissions in both CML lymphoid blast crisis and Ph$^+$ ALL are short-lived, typically lasting only 6 months.[5,11,13,14] At clinical relapse, such patients frequently, but not invariably, harbor dominant leukemic clones with drug-resistant KD mutations.[9,11,12] Whereas the addition of TKIs to conventional combination chemotherapy enhances remissions in Ph$^+$ ALL,[15,16] failure to eradicate minimal residual disease associated with the frequent evolution of BCR-ABL KD mutations remains a barrier to achieving long-term survival. Frequent *IKZF1* and *INK4A/B-ARF* deletions[2,3] likely contribute to the attenuated therapeutic response to BCR-ABL kinase inhibition.

Inactivation of the *Arf* tumor suppressor potently synergizes with p185$^{BCR-ABL}$ expression to generate a robust murine Ph$^+$ ALL model that recapitulates the biology and key genetic events described in the human disease.[17,18] This model relies on retroviral vector–mediated introduction of the p185$^{BCR-ABL}$ kinase into bone marrow progenitor cells derived from *Arf*-null C57Bl/6 mice, followed by short-term expansion of the transduced progeny under culture conditions that selectively support pre-B cell proliferation. After only 7-8 days of culture, arising polyclonal immature B-cell populations rapidly initiated lymphoid leukemia when inoculated intravenously into cohorts of nonconditioned, syngeneic mice. Remarkably, fewer than 20 *Arf*-null p185$^+$ donor cells (each genetically distinct and marked by both immunoglobulin heavy-chain gene rearrangements and unique sites of proviral insertion) induced fatal lymphoid leukemia in unconditioned healthy recipients within 30 days, implying that virtually every cell is a leukemia-initiating cell (LIC).[19] Although imatinib therapy induces sustained remissions in murine BCR-ABL–driven myeloproliferative disease[20] (ie, in "murine CML"), identical therapy only modestly improves the survival of mice harboring *Arf*-null, p185$^+$ ALL.[17,19] The initial resistance to imatinib therapy is non–tumor-cell–autonomous and depends on salutary effects conferred within the hematopoietic microenvironment.[19,21,22] With the goal of further understanding the mechanisms underlying the emergence of resistance to targeted antileukemic agents in vivo, we reengineered this murine Ph$^+$ ALL model to allow in vivo luminescent image–based tracking and quantification of leukemic-cell dissemination and therapeutic responsiveness. Using this high-throughput system, we have gained additional insights into the dynamic response to targeted and conventional therapies and have demonstrated that both KD mutation–dependent and –independent factors synergize to prevent the eradication of leukemia. By closely mimicking human Ph$^+$ ALL in its genetic and phenotypic properties, this model provides a powerful and economic experimental system for elucidating disease biology and for efficiently developing complex, combinatorial therapeutic strategies.

Methods

Retroviral expression vectors and virus production

A replication-defective mouse stem cell virus coexpressing human p185$^{BCR-ABL}$ and green fluorescent protein (GFP) was used, as described previously.[17,19] For in vivo luminescent imaging, the GFP cDNA cassette encoded from an internal ribosome entry site sequence was replaced by the *luc2* luciferase cDNA from the pGL4.10 vector (Promega).[18] Retroviral vectors were packaged into infectious, replication-incompetent ecotropic virions, as described previously.[23]

Bone marrow cell transduction, culture, and adoptive cell transfer

Mice were housed in an American Association of Laboratory Animal Care–accredited facility and were treated using institutional animal care and use committee–approved protocols in accordance with National Institutes of Health guidelines. Bone marrow cells from the long bones of *Arf* $^{-/-}$ mice[24] backcrossed onto a C57Bl/6 background were transduced with retroviral vector–containing supernatant and plated to derive BCR-ABL–transformed pre-B cells on autologous stroma.[17,25] After 7-8 days of culture, 2×10^5 *Arf*-null, BCR-ABL–expressing (p185$^+$), luciferase-positive (*luc*$^+$) pre-B LICs were further expanded for 2 days in culture in the absence of a stromal layer before cryopreservation. When required, LICs were thawed and recovered in liquid culture for 3 days before intravenous tail vein injection into cohorts of healthy, nonconditioned, immune-competent 10- to 12-week-old C57Bl/6J male mice (The Jackson Laboratory). Mice were observed daily and killed when moribund (dehydration, ruffled fur, poor mobility, respiratory distress). Survival curves were generated using GraphPad Prism Version 5.0 software, and the Mantel-Cox test was applied to pairwise comparisons of survival data.

Preclinical therapeutics

For in vivo use, dasatinib (LC Laboratories) was administered by oral gavage to recipient mice at 10 mg/kg per dose in 80mM citric acid (pH 3.1).[26] For combination studies, dexamethasone sodium phosphate injection solution (American Pharmaceutical Partners) was administered at 6 mg/L in drinking water for the first week and at 3 mg/L thereafter continuously.[27] Asparaginase (Elspar; Ovation Pharmaceuticals) was injected intraperitoneally once a week at 7500 IU/kg.[27] In all combinational therapeutic studies, a sulfamethoxazole (600 mg/L)/trimethoprim (120 mg/L) oral suspension (Baxter Healthcare) was added to drinking water for 3 days/wk, and 1000 mg/L of tetracycline (Sigma-Aldrich) was added 7 days/wk[27] from the start of therapy until 2 weeks after completion of treatment.

Bioluminescent imaging

Bioluminescent imaging and data analysis were performed using a Xenogen IVIS-200 system and Living Image Version 3.01 software (Caliper Life Sciences). Mice were injected intraperitoneally with D-luciferin (Caliper Life Sciences) at 100 mg/kg body weight and, after 3-5 minutes to allow substrate distribution, anesthetized for imaging using 2% isoflurane delivered at 2 L/min in O_2. Images were acquired using 1-minute exposures with small binning and with shortening of exposure times when signals were saturated. Total flux measurements (photons/second) were quantified over the whole-animal body or a contour drawn around a target organ. Images were normalized to the same color scale by setting maximum signal of luminescent activity to 1×10^6 photons/second/cm^2/steradian (sr). Recipient mice that remained clinically healthy for at least 3 months after completion of all therapy and whose hematopoietic tissues were completely free of any signs of detectable leukemia using in vivo imaging and sensitive in vitro luminescence assays were designated "long-term survivors."

In vitro luminescence activity

Luciferase activity was measured using a Bright-Glo Luciferase Assay System (Promega) and a Synergy 2 microplate reader (BioTek). Whole blood (100 μL after erythrocyte lysis performed with an FACS Lyse Wash Assistant; BD Biosciences) or 10^6 bone marrow cells in a 100-μL total volume were used to quantify disease burdens.

Analysis of BCR-ABL KD mutations

Genomic DNA was extracted with phenol-chloroform from hematopoietic tissues and leukemic-infiltrated meninges from moribund mice during therapy. Polymerase chain reactions to selectively amplify only the human

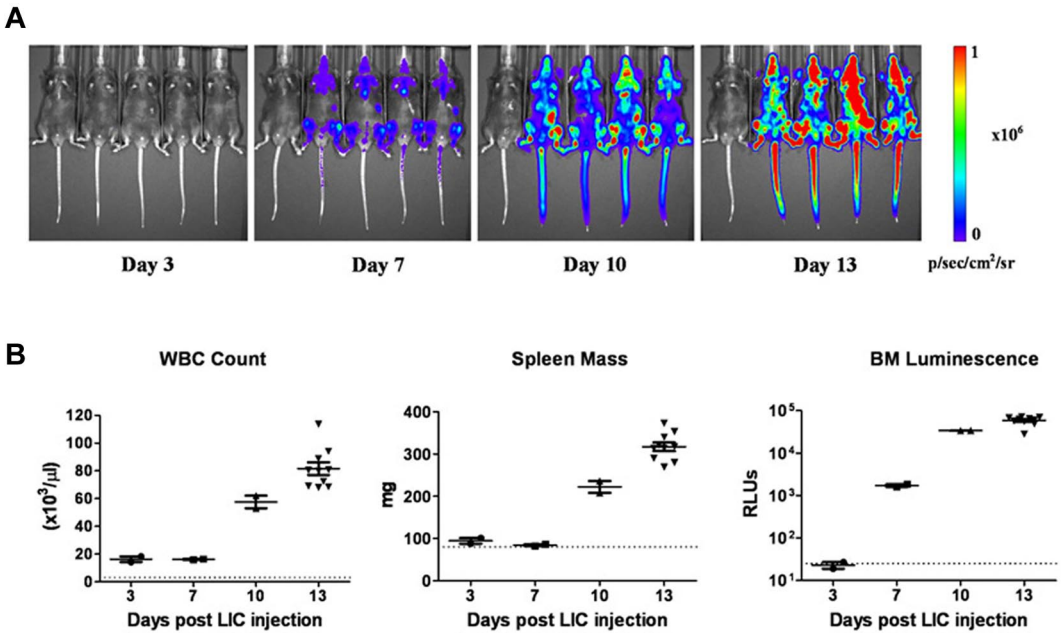

Figure 1. Progression of leukemia after adoptive transfer of LICs. (A) Serial whole-animal luminescent imaging of a representative cohort of recipient mice performed at different times after animals received intravenous injections of 2×10^5 *Arf*$^{-/-}$p185$^+$*luc*$^+$ LICs. Each panel includes a control, disease-free mouse (at far left) imaged under identical experimental conditions. All images are scaled to a maximum intensity of 1×10^6 photons (p)/s/cm^2/sr. Rapid increases in bioluminescence signals were noted with disease progression. (B) Randomly selected mice at 3, 7, and 10 days (n = 4 in each group) and at 13 days (n = 10) after injection of *luc*$^+$ LICs were euthanized, and determinations of white blood counts (WBC), spleen mass, and in vitro luminescence assays of bone marrow (BM) cell suspensions, expressed as relative light units, were performed. The dotted lines at the bottom of each graph represent the upper limits of normal WBC values (left) and spleen masses (middle) for age-matched male C57BL/6J mice, and the lower limit of sensitivity of the in vitro bone marrow cell luminescence assay (right). Median values are represented by solid horizontal lines and standard errors of the mean by brackets.

(and not the murine) *ABL* KD were performed as described previously.[7] Sequence analysis was performed on 10-20 independent bacterial colonies. Identified mutations were considered significant if present at ≥ 20% occurrence in individually sequenced clones.[7]

Histopathologic examination

Animals were anesthetized, perfused with 10 mL of phosphate-buffered saline, and dissected tissues were fixed in 10% neutral-buffered formalin for 24 hours and embedded in paraffin before sectioning. Sterna, tibiae, femora, whole heads, and spinal cords were decalcified using a Shandon TBD-2 decalcifier (Thermo Fisher Scientific) before embedding. Pathologic review of hematoxylin and eosin–stained sections (4 μm) was performed blinded to the experimental design and outcome.

Results

Dasatinib therapy induces remissions in murine Ph+ ALL

To dynamically monitor disease progression and responses to therapy in vivo, we substituted a luciferase reporter gene for the previously used GFP cDNA in the vector to generate otherwise genetically identical *Arf* $^{-/-}$p185$^+$*luc*$^+$ LICs. Preliminary experiments[18] demonstrated that after intravenous injection of 2×10^5 donor cells into healthy recipient mice (1) there was a significant consistency of luminescent signaling among cohorts of animals analyzed at the same intervals after transplant; (2) an average log increase in signal intensity was observed every 3 days, in agreement with previously determined kinetics of donor-cell expansion in vivo[17]; and (3) there was a 3-log dynamic range between barely detectable disease 3 days after transplantation and that encountered in moribund animals 10 days later (day 13). Despite the rapid expansion of *luc*$^+$ LICs in all hematopoietic tissues, including blood, spleen, and bone marrow (Figure 1A-B), recipient mice only developed clinical signs of leukemia (reduced mobility, ruffled fur) 11 days after receiving LICs. By day 13, however, average whole-animal luminescent signals of 2.4×10^8 photons/s were detected, and all recipient mice were profoundly moribund, with impaired mobility, hind-limb paralysis, pale appearance, and doming of the skull that required euthanasia. By all criteria, including LIC proliferation rates in culture, drug sensitivity, and in vivo leukemogenic activity, GFP$^+$ and *luc*$^+$ LICs were biologically equivalent.

When tested on cultured *Arf* $^{-/-}$p185$^+$ LICs, the 50% growth inhibitory concentration (IC_{50}) of dasatinib was nearly 1000-fold less than that of imatinib (0.1 vs 100nM, respectively; supplemental Figure 1, available on the *Blood* Web site; see the Supplemental Materials link at the top of the online article).[28,29] We therefore applied luminescent imaging to monitor dasatinib responses in animals bearing increasingly greater leukemic burdens at the start of therapy. Beginning 3, 7, or 10 days after recipients received 2×10^5 *Arf* $^{-/-}$p185$^+$*luc*$^+$ LICs, cohorts of mice were placed on continuous, twice-daily dasatinib therapy (10 mg/kg per dose) or were administered a vehicle control solution during a 4-week treatment window (Figure 2). Serial, weekly luminescent imaging demonstrated that all but one of the day 3 recipients had undetectable signals during and after dasatinib administration (Figure 2A). Dasatinib induced significant initial responses in all recipients in the day 7 and day 10 groups. However, many day 7 recipients maintained residual luminescent signals during therapy, and 6 of 19 of these mice relapsed (Figure 2B,D). All day 10 recipients initially responded to therapy, with an approximately 20-fold decrease in luminescent signals after 1 week, but 16 of 17 mice relapsed promptly when therapy was discontinued (Figure 2C-D). Increases in luminescent signals preceded clinical relapses by

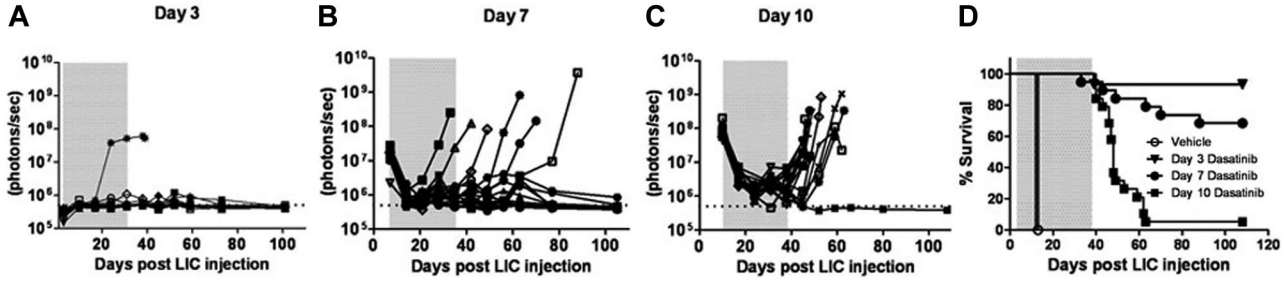

Figure 2. Dasatinib therapy initiated at different times after leukemia initiation determines response to therapy. Weekly whole-animal luminescent imaging of recipients of 2×10^5 *Arf* $^{-/-}$p185$^+$*luc*$^+$ LICs were acquired over the course of a 4-week dasatinib treatment window (depicted by gray shading in each panel) and thereafter at indicated intervals until clinical relapse or termination of the experiment. Dasatinib therapy was begun in 3 cohorts of recipient mice that had acquired progressively increased leukemic burdens 3 (A), 7 (B), or 10 (C) days after receipt of LICs (Figure 1). Whole-animal luminescent signals (photons/s/cm^2/sr) for each recipient mouse are plotted as solid lines that depict image intensity (ordinate) versus time in days after injection of LICs (abscissa). The empirically determined lower limit of sensitivity for whole-animal luminescence, derived from imaging of control nonleukemic animals, is indicated by the dotted line at the bottom of each panel. (D) Kaplan-Meier curves summarizing overall leukemia-free survival in each of the 3 cohorts of mice that received 4 weeks of continuous twice-daily (10 mg/kg/dose) dasatinib therapy.

1-3 weeks (Figure 2A-C vs Figure 2D). BCR-ABL mutational analysis revealed that 5 of the 18 mice (28%) that underwent relapse after discontinuation of dasatinib therapy had detectable KD mutations (all T315I) in at least 2 independent leukemic-infiltrated tissues (supplemental Figure 2). No KD mutations were detected in leukemic animals that rapidly died after treatment with vehicle alone. These studies demonstrated the utility of noninvasive luminescent imaging in monitoring leukemic progression, in quantifying responses to therapy, and in predicting clinical relapse, and highlighted the fact that clinically relevant KD mutations could arise in vivo after dasatinib exposure, drug discontinuation, and clinical relapse.

Dasatinib-refractory cells can rapidly yield leukemic clones with BCR-ABL KD mutations

Arf $^{-/-}$p185$^+$GFP$^+$ LICs that lack BCR-ABL KD mutations can persist in the hematopoietic microenvironment even in the face of maximally tolerated imatinib treatment regimens, and drug resistance in this setting is non–tumor-cell–autonomous and mediated, at least in part, by salutary effects of local cytokines.[19,22] Indeed, the absence of detectable BCR-ABL KD mutations in the majority of mice that underwent relapse after discontinuation of dasatinib after 4 weeks of therapy and in all untreated animals that died rapidly (Figure 2 and supplemental Figure 2) reinforced the conclusion that leukemic clones with KD mutations are not likely to be present at significant frequency during the early targeted treatment phase to prevent drug-induced eradication of LICs.

To more fully characterize the initial response to targeted therapy, we generated mice with high leukemic burdens and then performed serial analyses of dasatinib-treated recipients during induction of remission. Separate cohorts of mice were killed before the start of therapy 10 days after injection of LICs; after 1, 2, or 3 completed weeks of subsequent twice-daily dasatinib therapy; from an independent cohort of diseased, vehicle-treated mice; and from a cohort of animals that exhibited dasatinib-resistant, relapsed leukemias emerging after 38-67 days of continuous therapy (Figure 3A). As noted previously (Figure 2C), in vivo luminescent imaging revealed consistently significant responses within 1-2 weeks of initiation of twice-daily 10 mg/kg doses of dasatinib therapy, followed by persistence and modest expansion of residual drug-refractory *luc*$^+$ cells during the next 2 weeks of treatment (Figure 3A). In vitro luciferase activity measurements performed with recovered (red cell–deficient) whole-blood (Figure 3B) and bone marrow–cell suspensions (Figure 3C) revealed an initial 100-fold, dasatinib-dependent reduction in disease at these sites, roughly paralleling the response observed with whole-animal imaging. Bioluminescent activity measured ex vivo from dissected spleens (Figure 3D) and cervical lymph nodes (Figure 3E) showed similar trends in the timing of dasatinib-dependent effects, although residual leukemic cells within lymph nodes appeared to be the most refractory to dasatinib therapy, based on the absolute magnitude of the reduction in signals. In any single relapsed recipient mouse, there was typically a significant positive correlation between the extent of diminution of the whole-animal imaging-signal intensity, the luminescent intensities of hematopoietic tissues, and the extent of leukemic infiltration as determined by histopathologic examination.

We next determined the frequency of detectable KD mutant clones accumulating in drug-refractory leukemic populations from selected tissues of untreated, vehicle-treated, and short-term dasatinib-treated mice. Within the initial 1- to 2-week treatment window in which the abundance of drug-refractory LICs either reached a nadir or was only modestly expanding, 31 of 40 tissues from 14 mice, including all lymph node and meningeal samples, were free of cells bearing detectable KD mutations (supplemental Table 1). Likewise, KD mutations were neither detected in leukemic recipients before dasatinib therapy (24 leukemic tissues recovered from 8 mice) nor in vehicle-treated animals (20 tissues from 7 mice; supplemental Table 1). However, T315I mutations were detected in 9 individual tissues from 8 of 14 mice even during the first 2 weeks of dasatinib induction therapy. With one exception, these mutations were only identified in one tissue per animal (of 2-4 sampled tissues per recipient) and typically comprised a minority ($< 50\%$) of human ABL alleles that were recovered in cases bearing such mutant clones. At clinical relapse, however, 86% of dasatinib-resistant leukemias harbored abundant T315I alleles, usually in 2 or 3 separate hematopoietic tissues (Figure 4 and supplemental Figure 3). Therefore, dasatinib can rapidly select in vivo for the emergence of BCR-ABL KD mutant clones that later expand to dominate many drug-resistant leukemias at relapse.

Dasatinib treatment intensity selects for emergence of different KD mutations

To explore the relationships among intensity of dasatinib therapy, therapeutic response, recipient survival, and the emergence of BCR-ABL KD mutations, we inoculated recipient mice with 2×10^5 *Arf* $^{-/-}$p185$^+$*luc*$^+$ LICs, waited 10 days for them to

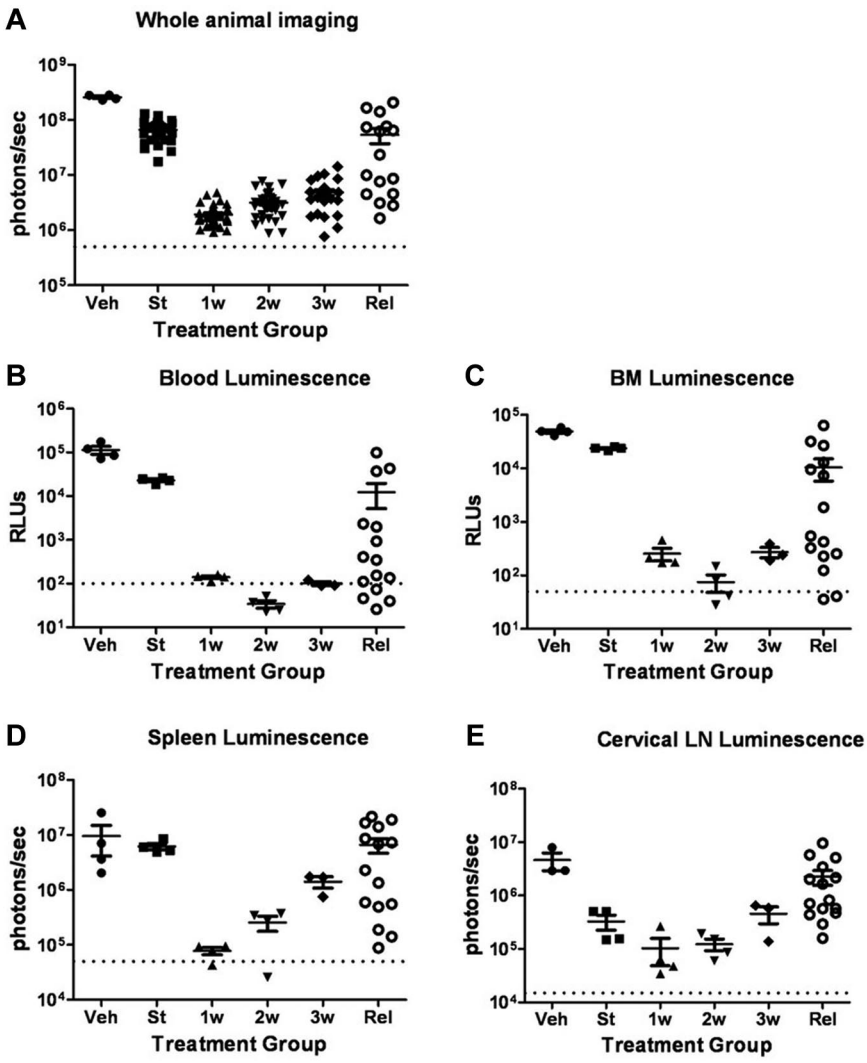

Figure 3. Dasatinib therapy induces initial responses followed by clinical relapses. (A) Whole-animal luminescent signals (photons/s/cm^2/sr) from recipient mice that received 2×10^5 *Arf*$^{-/-}$p185$^+$*luc*$^+$ LICs were acquired at the start (St) of dasatinib therapy 10 days after injection of LICs (n = 36). Serial images were obtained 1 week (1w; n = 37), 2 weeks (2w; n = 31), or 3 weeks (3w; n = 27) after twice-daily (5 days per week) dasatinib therapy or at clinical relapse (Rel; n = 16). For comparison, the imaging signals obtained from moribund, vehicle-treated mice (Veh; n = 4) are also presented. Median values ± standard errors are indicated by horizontal lines and brackets, respectively. (B-E) Quantitative in vitro luminescence intensities plotted as relative light units (RLUs, ordinate) were performed on 100 μL of erythrocyte-free whole blood (B) and 1×10^6 suspended bone marrow (BM) cells (C) prepared from representative mice taken from cohorts depicted in panel A. In situ spleen (D) and cervical lymph node (LN) luminescence signals (E) recorded in photons/second (ordinate) were acquired from intact whole tissues. Four mice were analyzed in each group (except Rel, where n = 15). Values in panels B-E are presented as median ± SE. The empirically determined lower limits of sensitivity are indicated by dotted lines at the bottom of the panels.

develop a significant disease burden, and randomized them to 1 of 4 dasatinib treatment arms (all at 10 mg/kg/dose): (1) twice daily 7 days per week, (2) twice daily 5 days per week; (3) once daily 7 days per week; and (4) once daily 5 days per week. Compared with the rapid demise of vehicle-treated control mice, successive increases in dasatinib intensity progressively prolonged recipient survival (Figure 4A). However, despite therapeutic efficacy, 32 of 34 mice ultimately relapsed while maintained on therapy, one additional mouse relapsed after discontinuation of treatment, and only a single mouse survived until the completion of the experiment. Thus, as in human Ph$^+$ ALL, mice bearing significant tumor burdens entered remission, remained free of clinical signs of disease for an extended period of time, but ultimately failed dasatinib therapy.

Within the first 2 weeks after initiating treatment, twice-daily and once-daily dasatinib typically induced an average 30-fold and 10-fold reduction in whole-animal luminescent signals, respectively (Figure 4B-E). Nonetheless, virtually all recipients exhibited residual drug-refractory disease in the head and neck region (including cervical lymph nodes), whereas mice treated once daily also exhibited residual bone marrow disease (see representative inset images in Figure 4B,E). Again, significant increases in luminescent signals often predated clinical relapse by several weeks, but the phenotype of drug-resistant leukemia, characterized by heavy leukemic infiltration of spleen, bone marrow, elevated white blood counts, and disseminated lymphadenopathy, was similar in all treatment groups.

After prolonged dasatinib exposure, BCR-ABL KD mutations were detected at clinical relapse in the majority of drug-resistant leukemias from all treatment groups. In 26 of 29 mice receiving twice-daily dasatinib treatment, T315I mutations predominated in independent hematopoietic tissues (Table 1 and supplemental Figure 3). However, 5 relapsed mice in these cohorts also harbored leukemic clones with discrete P-loop mutations (Table 1 and supplemental Figure 3). Less-intensive and less-efficacious once-daily dasatinib therapy was associated with fewer mutations overall (9 of 14 mice), less-frequent infiltration of multiple tissues with leukemic clones containing mutant KD alleles, and a significantly greater proportion of P-loop versus T315I mutant alleles in relapsed leukemias (Table 1 and supplemental Figure 3). These findings imply that the overall level of exposure to dasatinib determines the frequency of recovery of leukemic clones bearing different KD mutations, with T315I mutations being preferentially selected in response to high-dose drug administration. Readapting leukemic cells exhibiting T315I mutations to short-term (1-2 week) culture strongly selected against the frequency of colonies harboring mutant alleles, indicating that polymerase chain reaction analysis of fresh tumor material was mandatory.

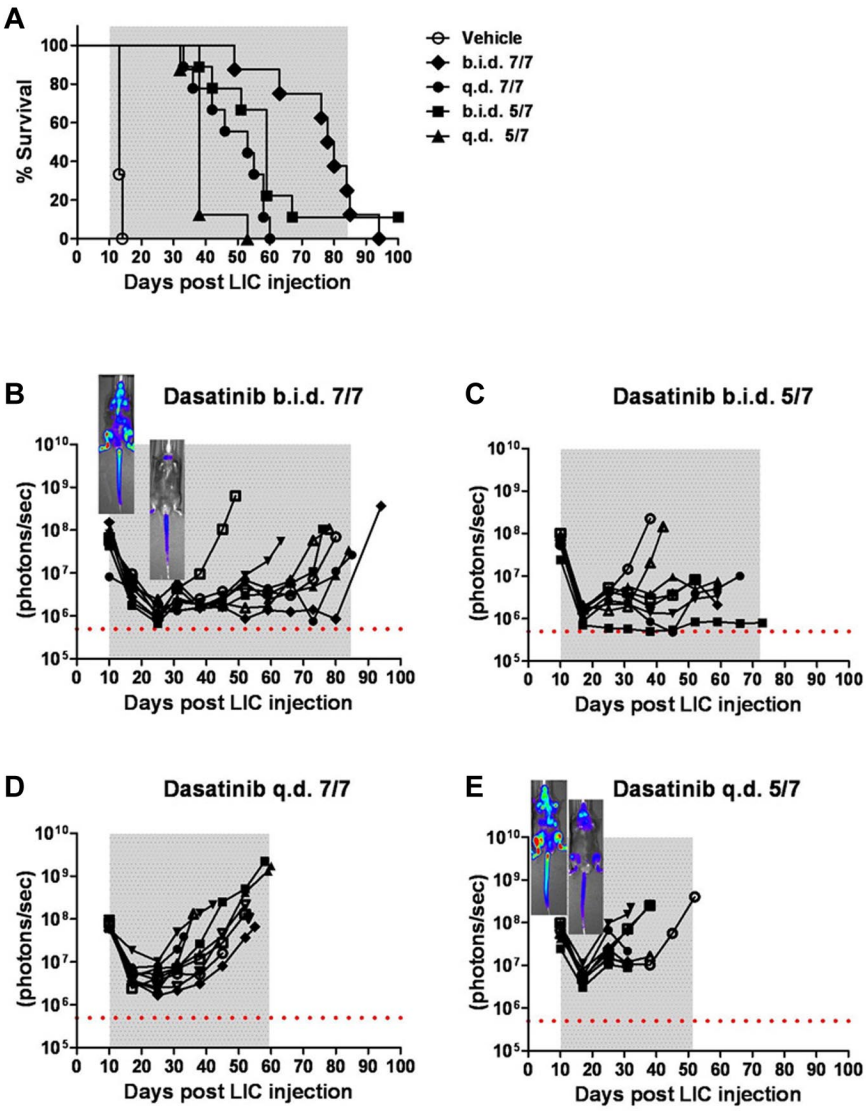

Figure 4. Intensity of dasatinib therapy correlates with enhanced survival but fails to provide durable remissions when initiated in mice harboring high leukemic burdens. (A) Kaplan-Meier curves representing the overall survival of 4 cohorts of recipient mice that received 2×10^5 *Arf* $^{-/-}$p185$^+$*luc*$^+$ LICs 10 days before the start of dasatinib therapy (n = 8 per treatment arm). As indicated in the inset legend, mice received vehicle alone, twice-daily dasatinib therapy 7 days per week (b.i.d. 7/7) or 5 days per week (b.i.d. 5/7), or once-daily dasatinib therapy 7 days per week (q.d. 7/7) or 5 days per week (q.d. 5/7). (B-E) Ten days after LIC inoculation, mice in each cohort evidenced similar degrees of advanced disease as determined by image signal intensities. Whole-animal luminescent signals (photons/s/cm^2/sr) for individual recipient mice are plotted as solid lines that depict image intensity (ordinate) versus time in days after injection of LICs (abscissa). The empirically determined lower limit of sensitivity for whole-animal luminescence is indicated by the dotted horizontal line at the bottom of each panel. Therapy was continued throughout the intervals designated by gray shading. Representative inset images reveal localized disease in the neck area (cervical lymph nodes) in the twice-daily 7/7 treatment group (B), in contrast to the disseminated disease including the hind limbs (bone marrow compartment) in the once-daily 5/7 cohort (E).

Meningeal leukemia contributes to clinical relapse after prolonged dasatinib therapy

Although dasatinib-resistant leukemias at relapse were frequently associated with signs of widely disseminated disease, a significant number of recipients failed therapy, with disease primarily localized to the head and neck region (supplemental Figure 4); these mice displayed a hunched posture, domed skull, hyperactivity, and intermittent generalized seizures, all consistent with intracranial leukemia and/or increased intracranial pressure. These central nervous system (CNS)–centered relapses were almost invariably associated with lower white blood cell counts, smaller spleen sizes, less bone marrow infiltration, and absent or low levels (< 50%) of T315I alleles in residual bone marrow leukemic blasts.

Table 1. Intensity of dasatinib therapy influences the emergence of BCR-ABL KD mutations in relapsed animals

		Mutational frequency, % of mice	
Treatment group	**Median survival, d**	**T315I**	**P-loop**
Twice daily, 7 d/wk (n = 8)	79	88	0
Twice daily, 5 d/wk (n = 21)	59	86	33
Once daily, 7 d/wk (n = 8)	53	50	25
Once daily, 5 d/wk (n = 6)	38	16	50

Bone marrow, spleen, and cervical lymph nodes from animals that relapsed on continuous dasatinib therapy were analyzed for the presence of KD mutations. The frequency of the T315I mutation decreased with the reduced intensity of dasatinib treatment, whereas P-loop mutations were more commonly detected in mice receiving less intensified dasatinib schedules. In 3 separate leukemias in which both T315I and P-loop mutations were detected in the same tissue, both mutations were absent on the same sequenced amplicon, suggesting that they arose in independent leukemic clones rather than sequentially during the course of therapy. The tissues and nature of different KD mutations detected in individual mice within the 4 treatment arms are summarized in detail in supplemental Figure 3.

Blinded histopathologic examination of tissues at relapse confirmed significant leukemic infiltration of the meninges in all animals, whether they failed with disseminated or CNS-centered disease (Figure 5). In some cases, leukemic cells invaded the brain parenchyma. Sequential analyses of CNS leukemia in dasatinib-naive and dasatinib-treated recipients (performed in parallel with the studies described in Figure 3) revealed that the meningeal infiltration detectable at the start of therapy (Figure 5B) rapidly progressed without treatment (Figure 5A), whereas dasatinib therapy effectively controlled meningeal leukemia during the first week of therapy (Figure 5C), only to lose its antileukemic activity over the next 2 weeks until inevitable relapse ensued (Figure 5D). Almost identical patterns of initial dasatinib response followed by

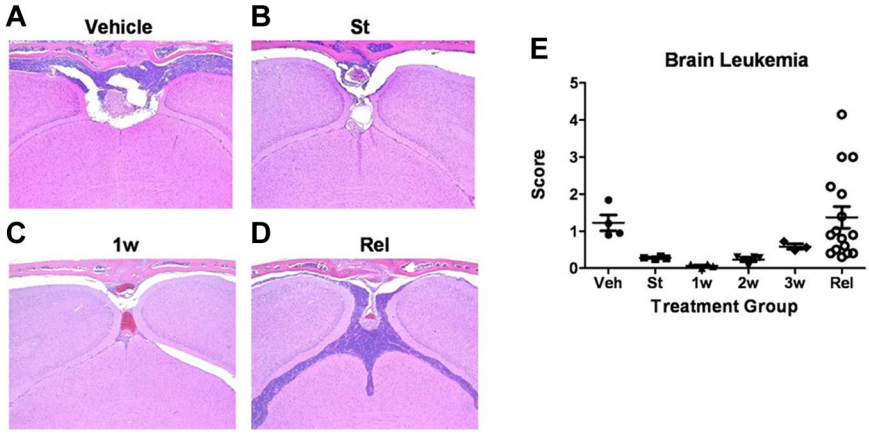

Figure 5. Leukemia-cell infiltration into the brain. (A-D) Formalin-fixed, decalcified, paraffin-embedded sections from the heads of mice were stained with hematoxylin and eosin and examined for the presence of leukemic infiltration of meninges, brain parenchyma, and bone marrow within the overlying calvaria. (A) Coronal sections from moribund, vehicle-treated mice 13 days after receipt of LICs showed characteristically high levels of leukemic-cell infiltration into the meningeal layer associated with filling of bone marrow space in overlying calvaria. (B) At the start (St) of dasatinib therapy 10 days after LIC injection, recipients typically harbored detectable leukemic infiltrates in the meninges. (C) Infiltrates decreased significantly after 1 week (1w) of dasatinib therapy. (D) Significant leukemic expansion was observed in all mice that ultimately relapsed despite continuous dasatinib therapy. (E) Leukemia infiltration of the CNS of recipients was reviewed and scored by a blinded veterinary pathologist from mice at the start of dasatinib therapy (St; n = 4); after 1 week (1w; n = 4), 2 weeks (2w; n = 4), or 3 weeks (3w; n = 4) of twice-daily (5 days per week) dasatinib therapy; or at clinical relapse (Rel; n = 15). This panel depicts the leukemic infiltration score in mice at the indicated times; scores represent the thickest portion of lymphocyte infiltration of all sections reviewed and are expressed in micrometers.

clinical failure were observed by histopathologic examination of the dissected spinal cords (sampled at 3 spinal levels) from recipient mice. Thus, leukemic disease in the CNS, primarily in the meninges, contributed to the clinical deterioration and demise of dasatinib-treated animals whose systemic disease remained otherwise well-controlled.

Dexamethasone and L-asparaginase improve dasatinib control of murine Ph+ ALL

We tested whether the addition of one or 2 "conventional" anti-ALL chemotherapeutic agents to a dasatinib-containing regimen would enhance initial disease control during induction and lead to improved survival. We compared the preclinical activity of dasatinib with the antilymphoid leukemic agents dexamethasone and L-asparaginase[27,30] at the initiation of therapy in recipients bearing very significant leukemic burdens (ie, 10 days after receiving 2×10^5 LICs). Dexamethasone and L-asparaginase are widely used in the treatment of ALL, act through different mechanisms, have nonoverlapping toxicities, and, when combined with TKIs, result in impressive responses in adults.[15,16,30] In 7 independent treatment arms, typically with 16 mice per cohort, these drugs were administered alone or in all possible combinations. The plasma concentrations of dexamethasone and L-asparaginase achievable in mice with the dosing schedules used are at least as high as those used in human patients and have previously proven efficacious.[27] Weekly L-asparaginase treatment demonstrated no single-agent antileukemic activity (Figure 6A-B), yielding a median survival of 14 days compared with 13 days for the vehicle-treated group. Oral dexamethasone enhanced survival relative to controls (median 17 days, $P = .0043$) and controlled disease in several mice (Figure 6A-C), albeit less effectively than once-daily dasatinib therapy (median survival 31 days, $P < .0001$; Figure 6A,D). In pairwise combinations, the combined administration of L-asparaginase and dexamethasone did not further enhance dexamethasone-dependent survival (Figure 6A). Despite possessing modest single-agent activity, both L-asparaginase ($P < .0001$) and dexamethasone ($P = .0008$) significantly enhanced the depth and length of dasatinib-induced remissions (Figure 6A,F), increased the lengths of median survival (40 and 80.5 days for dasatinib/L-asparaginase and dasatinib/dexamethasone groups, respectively), and ultimately yielded some long-term survivors (Figure 6A). The combination of all 3 agents provided the greatest antileukemic activity, rapidly inducing remissions in all recipients, which translated to long-term survival in 9 of 16 mice (Figure 6A,G).

Treatment groups that received both dasatinib and dexamethasone or the 3-drug combination typically developed clinical signs of CNS leukemia that required euthanasia despite very effective systemic control of their disease (supplemental Figure 5). In contrast, all other treated mice relapsed with more disseminated disease. Unlike mice that relapsed on single-agent dasatinib therapy, and consistent with better disease control, animals receiving dasatinib together with other agents exhibited less frequent BCR-ABL KD mutations (46% vs 86%) that were generally limited to a single hematopoietic tissue. However, analysis of representative meningeal tumor material from mice that relapsed on combined dasatinib and L-asparaginase (7 mice), dasatinib and dexamethasone (2 mice), or all 3 drugs (2 mice) showed no evidence of KD mutations, suggesting that other nonmutational mechanism(s) also contribute to therapeutic resistance in the CNS. Thus, the addition of well-tolerated and well-characterized antileukemic chemotherapeutics to dasatinib therapy dramatically enhanced remission induction and induced sustained and durable remissions in a majority of recipient animals.

Discussion

The combination of BCR-ABL expression and *Arf* inactivation in pre-B cells models 2 key genetic lesions of human Ph+ ALL[3] and allows the generation of polyclonal populations of cultured LICs capable of rapidly inducing Ph+ ALL in healthy syngeneic mice.[17,19] Although the majority of human Ph+ ALLs also sustain *IKZF1* (*IKAROS*) mutations, decreased IKZF1 levels arrest cells at the pre–B-cell stage,[4] an outcome mimicked by the short-term culture conditions used in our system to generate LICs.[25]

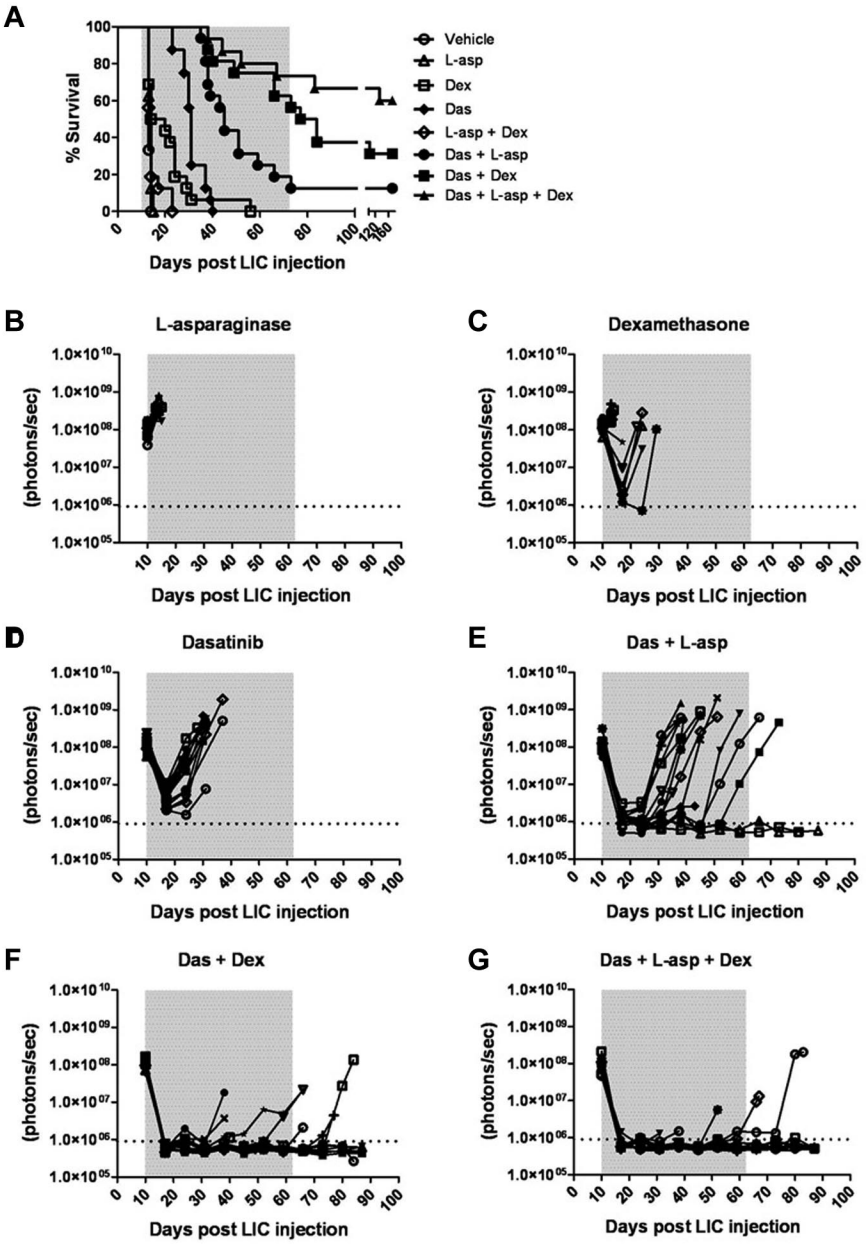

Figure 6. Dexamethasone and L-asparaginase therapy prolongs dasatinib-induced remissions and enhances survival of leukemic mice. (A) Kaplan-Meier curves summarizing the overall survival of cohorts of leukemic mice receiving vehicle alone, single agents, or different drug combinations (as indicated in the inset panel). Each treatment arm included 16 mice. Therapies were initiated 10 days after mice received 2×10^5 LICs. The addition of L-asparaginase (L-asp), dexamethasone (Dex), or both to dasatinib (Das) therapy significantly prolonged median survival of recipients (*P* values in text), and was associated with long-term survival of 13% (n = 2), 31% (n = 5), and 56% (n = 9) of mice in these respective treatment groups. (B-G) Whole-animal luminescent signals (photons/s/cm^2/sr) from individual leukemic mice were serially acquired to monitor therapeutic responses and subsequent relapses. In all graphs, signals from individual recipient mice are plotted as solid lines that depict imaging intensity (ordinate) versus time in days after injection of LICs (abscissa). The empirically determined lower limit of sensitivity for whole-animal luminescence is indicated by the dotted horizontal line at the bottom of each graph, and the indicated treatment periods for single or multiple agents are shaded in gray.

Inactivation of the *Arf* tumor suppressor in donor LICs circumvents the need to irradiate or otherwise condition recipient mice, a required feature of most mouse leukemia models, and instead allows ALL to develop in animals that retain an intact hematopoietic and immune system, more closely modeling the human disease.[17] Because only 20 p185$^+$, *Arf*-null LICs can induce fatal disease within 30 days of their administration into naive syngeneic recipients, and because many millions of such cells can be generated from relatively few bone marrow progenitors in a short-term (7-8 days) selective culture system, it now becomes possible to study Ph$^+$ ALL induction, progression, and responses to different therapeutic modalities in large cohorts of normal recipient animals at a relatively modest cost. Stable and relatively uniform expression of the *luc2* marker gene in all transduced LICs permits quantitative visualization of leukemic progression and therapeutic response in living mice, as well as enabling very sensitive ex vivo assessments of leukemic-cell infiltration of tissues recovered from diseased animals. Given that even potent, second-generation targeted inhibitors of BCR-ABL kinase do not induce durable remissions in patients with Ph$^+$ ALL, and considering the difficulties of piloting complex therapeutic combinations in human clinical trials, this robust, high-throughput, and economic mouse model affords many potential advantages for relevant preclinical investigations.

Under conditions in which maximally tolerated doses of imatinib demonstrated very modest in vivo therapeutic efficacy in *Arf*-null, p185$^+$ leukemias,[19] single-agent dasatinib therapy potently induced remissions, controlled leukemic progression, and significantly enhanced recipient survival, as described previously for human patients.[11,30] Factors that likely account for dasatinib's greater efficacy include its expanded target kinase profile to include the SRC family of nonreceptor TKs,[31] its ability to achieve peak plasma levels of drug approaching 100nM (approximately1000-fold more than the in vitro IC_{50} for these LICs),[32,33] and the recognition that even transient dasatinib

(but not imatinib) exposure irreversibly commits BCR-ABL–driven lymphoid cells to undergo apoptosis.[34,35]

BCR-ABL KD mutations are a frequent, but not requisite, accompaniment to the development of resistance to TKIs.[7,36,37] The T315I KD mutation dominated many, but not all, relapsed dasatinib-treated mice, paralleling its frequent appearance at relapse of TKI-treated human BCR-ABL–driven lymphoid leukemias. Our consistent inability to detect expansion of leukemic clones bearing KD mutations in dasatinib-naive animals implies that few if any cells with preexisting KD mutations are present in cultured donor *Arf*$^{-/-}$p185^{+} LICs, and that such cells, even if present at very low abundance, provide no proliferative advantage in the absence of TKI treatment. Only over the course of 2 weeks of dasatinib "induction" therapy, during which time $> 99\%$ of BCR-ABL–expressing cells were eradicated (equivalent to the observed 2 to 3-log reduction in leukemia burden), did KD mutant–expressing populations emerge at detectable levels in hematopoietic tissues recovered from some, but not all, animals.

When dasatinib therapy was initiated in recipient mice whose disseminated leukemic burden approached that typically observed at diagnosis in human Ph^{+} ALL patients, the intensity (ie, frequency) of dasatinib monotherapy determined the magnitude of the initial response, the duration of remission, and the spectrum of KD mutations at relapse. More intensive therapy, in which T315I mutations predominated and less-intensive regimens more often associated with P-loop mutations, apparently apply differential selective pressures to yield KD alleles that either confer more complete or subtle dasatinib resistance, respectively. The significantly lower KD mutation frequency observed at relapse in recipient mice that received a shorter treatment is consistent with the idea that dasatinib therapy functions to both select and maintain KD mutations in vivo. Different BCR-ABL mutations impart distinct biologic effects.[38-40] For example, some P-loop mutations augment the constitutive levels of TK activity to increase oncogenicity, whereas the T315I mutation does not confer an intrinsic proliferative advantage but instead promotes resistance to a broad spectrum of TKIs. However, the lack of BCR-ABL KD mutations in many dasatinib-refractory cells at the end of induction underscores previous findings that tumor-cell–extrinsic factors in the hematopoietic microenvironment, such as host cytokines, heterotypic cell-cell interactions, and local drug accessibility, independently contribute to drug resistance at these early stages.[19,21,22]

CNS relapse in Ph^{+} lymphoid leukemias remains a significant clinical problem. Despite the ability of imatinib to effectively control CML and to transiently suppress the progression of systemic Ph^{+} ALL, increasingly frequent CNS relapse after imatinib therapy[20,41-43] reflects its poor penetration into the cerebrospinal fluid.[44] Dasatinib can cross the blood-brain barrier, and accumulates at 3%-9% of plasma levels in preclinical murine studies and at 5%-28% of plasma levels in human leukemic patients, which is thought to contribute to significant clinical responses of Ph^{+} ALL patients to dasatinib single-agent or combination therapy.[45] At the start of therapy, murine Ph^{+} ALL exhibited significant CNS disease, both in the meninges and spinal cord. However, dasatinib's antileukemic control within the CNS was not efficacious in our model system, and was limited to the first weeks of therapy, beyond which leukemia expansion progressed during the remaining course of treatment. High rates of CNS relapse were observed on continuous and maximally intensive dasatinib therapy with examples of "isolated" CNS relapse despite good systemic control. Dasatinib exhibited substantial antitumor activity in an intracranial CML mouse model with significantly increased survival rates, although it failed to eradicate CNS disease completely.[45] Drug access influenced by transporter molecules within the blood-brain barrier may be relevant.[46] Conceivably, as in Notch-driven T-ALL, chemokine-signaling mechanisms activated by BCR-ABL might facilitate CNS invasiveness.[47]

In human Ph^{+} lymphoid leukemia, maximally intensive dasatinib therapy produces a stereotypical triphasic response composed of an initial induction of remission, a maintenance phase, and inevitable, but less predictable, clinical relapse.[11,48] The addition of dasatinib to cytotoxic chemotherapy has recently proven more effective in achieving longer-term remissions.[15] The positive, albeit incomplete, response to dasatinib therapy encouraged us to implement additional combinational preclinical drug trials in conjunction with 2 other antileukemic agents, dexamethasone and L-asparaginase. These 2 drugs, already used to treat Ph^{+} ALL, have different mechanisms of action, exhibit nonoverlapping toxicities, and improve clinical responses to TKIs.[15,16] Although cerebrospinal fluid dexamethasone levels are not limited by the blood-brain barrier[49] and are efficient in the treatment of meningeal leukemia,[50] most relapsed mice still exhibited isolated CNS disease on combination therapy. In 11 mice that failed therapy with dasatinib plus L-asparaginase, dexamethasone, or both, BCR-ABL KD mutations were not detected in leukemic cells freshly harvested from the CNS, suggesting that drug resistance is conveyed through other mechanisms. Nonetheless, the use of both agents together with dasatinib enhanced the induction response, increased the duration of remission, and led to a significantly increased long-term survival rate (60% in the cohort of mice receiving triple treatment).

In summary, our mouse model recapitulates key features of human Ph^{+} ALL. Specifically, (1) the underlying genetic basis and phenotypic presentation of disease are similar; (2) LICs efficiently induce ALL in healthy, nonconditioned hosts; (3) mice with substantial leukemic burdens respond to, but ultimately fail, targeted therapy with dasatinib; (4) drug resistance reflects a confluence of mutational and host-dependent mechanisms; and (5) combinatorial therapy with targeted and conventional antileukemic agents extends long-term survival. Preclinical trials using multiple agents underscore the potential value of this murine Ph^{+} ALL model for efficiently and cheaply piloting combination therapies and for elucidating mechanisms of drug resistance, information that is much more difficult to extract from complex human clinical trials.

Acknowledgments

We thank Ryan Wilson and Shelly Wilkerson for assistance with mouse therapeutic studies, Melissa Johnson and Monique Payton for assistance with animal imaging, Richard A. Ashmun and Ann-Marie Hamilton-Easton for performing flow cytometric analysis, and Owen Witte (University of California Los Angeles) for the MSCV-BCR-ABL-IRES-GFP retroviral vector.

This work was supported in part by an American Association for Cancer Research (AACR) Centennial Career Development Award for Childhood Cancer Research (to R.T.W.), by National Institutes of Health grant R01 CA 142665 (to M.V.R.), by St Jude Comprehensive Cancer Center Core Grant CA-21765, and by the American Lebanese Syrian Associated Charities (ALSAC) of St Jude Children's Research Hospital. C.J.S. is an investigator at the Howard Hughes Medical Institute.

Authorship

Contribution: N.B. performed research, designed experiments, analyzed data, and prepared the manuscript; H.L.M. performed mutation analysis; C.R.C. implemented in vivo imaging; J.B.M. provided technical assistance; J.E.R. performed pathologic examination; and M.V.R., C.J.S. and R.T.W. designed experiments and prepared the manuscript.

Conflict-of-interest disclosure: The authors declare no competing financial interests.

Correspondence: Nidal Boulos, Department of Oncology, St Jude Children's Research Hospital, 262 Danny Thomas Pl, Memphis, TN 38105; e-mail: nidal.boulos@stjude.org.

References

1. Wong S, Witte ON. The BCR-ABL story: bench to bedside and back. *Annu Rev Immunol.* 2004;22:247-306.
2. Mullighan CG, Miller CB, Radtke I, et al. BCR-ABL1 lymphoblastic leukaemia is characterized by the deletion of Ikaros. *Nature.* 2008;453(7191):110-114.
3. Mullighan CG, Williams RT, Downing JR, Sherr CJ. Failure of CDKN2A/B (INK4A/B-ARF)-mediated tumor suppression and resistance to targeted therapy in acute lymphoblastic leukemia induced by BCR-ABL. *Genes Dev.* 2008;22(11):1411-1415.
4. Trageser D, Iacobucci I, Nahar R, et al. Pre-b-cell receptor-mediated cell cycle arrest in Philadelphia chromosome-positive acute lymphoblastic leukemia requires IKAROS function. *J Exp Med.* 2009;206(8):1739-1753.
5. Druker BJ, Talpaz M, Resta DJ, et al. Efficacy and safety of a specific inhibitor of the BCR-ABL tyrosine kinase in chronic myeloid leukemia. *N Engl J Med.* 2001;344(14):1031-1037.
6. Rousselot P, Huguet F, Rea D, et al. Imatinib mesylate discontinuation in patients with chronic myelogenous leukemia in complete molecular remission for more than 2 years. *Blood.* 2007;109(1):58-60.
7. Shah NP, Nicoll JM, Nagar B, et al. Multiple BCR-ABL kinase domain mutations confer polyclonal resistance to the tyrosine kinase inhibitor imatinib (STI571) in chronic phase and blast crisis chronic myeloid leukemia. *Cancer Cell.* 2002;2(2):117-125.
8. Bixby D, Talpaz M. Mechanisms of resistance to tyrosine kinase inhibitors in chronic myeloid leukemia and recent therapeutic strategies to overcome resistance. *Hematology Am Soc Hematol Educ Program.* 2009;461-476.
9. Hochhaus A, Kantarjian HM, Baccarani M, et al. Dasatinib induces notable hematologic and cytogenetic responses in chronic-phase chronic myeloid leukemia after failure of imatinib therapy. *Blood.* 2007;109(6):2303-2309.
10. Kantarjian H, Giles F, Wunderle L, et al. Nilotinib in imatinib-resistant CML and Philadelphia chromosome-positive ALL. *N Engl J Med.* 2006;354(24):2542-2551.
11. Talpaz M, Shah NP, Kantarjian H, et al. Dasatinib in imatinib-resistant Philadelphia chromosome-positive leukemias. *N Engl J Med.* 2006;354(24):2531-2541.
12. O'Hare T, Eide CA, Deininger MW. Bcr-Abl kinase domain mutations, drug resistance, and the road to a cure for chronic myeloid leukemia. *Blood.* 2007;110(7):2242-2249.
13. Alvarado Y, Apostolidou E, Swords R, Giles FJ. Emerging therapeutic options for Philadelphia-positive acute lymphocytic leukemia. *Expert Opin Emerg Drugs.* 2007;12(1):165-179.
14. de Labarthe A, Rousselot P, Huguet-Rigal F, et al. Imatinib combined with induction or consolidation chemotherapy in patients with de novo Philadelphia chromosome-positive acute lymphoblastic leukemia: results of the GRAAPH-2003 study. *Blood.* 2007;109(4):1408-1413.
15. Ravandi F, O'Brien S, Thomas D, et al. First report of phase II study of dasatinib with hyperCVAD for the frontline treatment of patients with Philadelphia chromosome positive (Ph+) acute lymphoblastic leukemia. *Blood.* 2010;116(12):2070-2077.
16. Schultz KR, Bowman WP, Aledo A, et al. Improved early event-free survival with imatinib in Philadelphia chromosome-positive acute lymphoblastic leukemia: a children's oncology group study. *J Clin Oncol.* 2009;27(31):5175-5181.
17. Williams RT, Roussel MF, Sherr CJ. Arf gene loss enhances oncogenicity and limits imatinib response in mouse models of Bcr-Abl-induced acute lymphoblastic leukemia. *Proc Natl Acad Sci U S A.* 2006;103(17):6688-6693.
18. Williams RT, Sherr CJ. The INK4-ARF (CDKN2A/B) locus in hematopoiesis and BCR-ABL-induced leukemias. *Cold Spring Harb Symp Quant Biol.* 2008;73:461-467.
19. Williams RT, den Besten W, Sherr CJ. Cytokine-dependent imatinib resistance in mouse BCR-ABL+, Arf-null lymphoblastic leukemia. *Genes Dev.* 2007;21(18):2283-2287.
20. Wolff NC, Richardson JA, Egorin M, Ilaria RL Jr. The CNS is a sanctuary for leukemic cells in mice receiving imatinib mesylate for Bcr/Abl-induced leukemia. *Blood.* 2003;101(12):5010-5013.
21. Sawyers CL. Where lies the blame for resistance–tumor or host? *Nat Med.* 2007;13(10):1144-1145.
22. Gregory MA, Phang TL, Neviani P, et al. Wnt/Ca2+/NFAT signaling maintains survival of Ph+ leukemia cells upon inhibition of Bcr-Abl. *Cancer Cell.* 2010;18(1):74-87.
23. Zindy F, Eischen CM, Randle DH, et al. Myc signaling via the ARF tumor suppressor regulates p53-dependent apoptosis and immortalization. *Genes Dev.* 1998;12(15):2424-2433.
24. Kamijo T, Zindy F, Roussel MF, et al. Tumor suppression at the mouse INK4a locus mediated by the alternative reading frame product p19ARF. *Cell.* 1997;91(5):649-659.
25. Whitlock CA, Witte ON. Long-term culture of murine bone marrow precursors of B lymphocytes. *Methods Enzymol.* 1987;150:275-286.
26. Hu Y, Swerdlow S, Duffy TM, Weinmann R, Lee FY, Li S. Targeting multiple kinase pathways in leukemic progenitors and stem cells is essential for improved treatment of Ph+ leukemia in mice. *Proc Natl Acad Sci U S A.* 2006;103(45):16870-16875.
27. Yang L, Boyd K, Kaste SC, Kamdem Kamdem L, Rahija RJ, Relling MV. A mouse model for glucocorticoid-induced osteonecrosis: effect of a steroid holiday. *J Orthop Res.* 2009;27(2):169-175.
28. O'Hare T, Walters DK, Stoffregen EP, et al. In vitro activity of Bcr-Abl inhibitors AMN107 and BMS-354825 against clinically relevant imatinib-resistant Abl kinase domain mutants. *Cancer Res.* 2005;65(11):4500-4505.
29. Shah NP, Tran C, Lee FY, et al. Overriding imatinib resistance with a novel ABL kinase inhibitor. *Science.* 2004;305(5682):399-401.
30. Pui CH, Evans WE. Treatment of acute lymphoblastic leukemia. *N Engl J Med.* 2006;354(2):166-178.
31. Lombardo J, Lee FY, Chen P, et al. Discovery of N-(2-chloro-6-methyl-phenyl)-2-(6-(4-(2-hydroxyethyl)-piperazin-1-yl)-2-methylpyrimidin-4-ylamino(thiazole-5-carboxamide (BMS-354825), a dual Scr/Abl kinase inhibitor with potent antitumor activity in preclinical assays. *J Med Chem.* 2004;47(27):6658-6661.
32. Luo FR, Yang Z, Camuso A, et al. Dasatinib (BMS-354825) pharmacokinetics and pharmacodynamic biomarkers in animal models predict optimal clinical exposure. *Clin Cancer Res.* 2006;12(23):7180-7186.
33. Kamath AV, Wang J, Lee FY, Marathe PH. Preclinical pharmacokinetics and in vitro metabolism of dasatinib (BMS-354825): a potential oral multitargeted kinase inhibitor against SRC and BCR-ABL. *Cancer Chemother Pharmacol.* 2008;61(3):365-376.
34. Shah NP, Kasap C, Weier C, et al. Transient potent BCR-ABL inhibition is sufficient to commit chronic myeloid leukemia cells irreversibly to apoptosis. *Cancer Cell.* 2008;14(6):485-493.
35. Snead JL, O'hare T, Adrian LT, et al. Acute dasatinib exposure commits Bcr-Abl-dependent cells to apoptosis. *Blood.* 2009;114(16):3459-3463.
36. Pfeifer H, Wassmann B, Pavlova A, et al. Kinase domain mutations of BCR-ABL frequently precede imatinib-based therapy and give rise to relapse in patients with de novo Philadelphia-positive acute lymphoblastic leukemia (Ph+ ALL). *Blood.* 2007;110(2):727-734.
37. Jones D, Thomas D, Yin CC, et al. Kinase domain point mutations in Philadelphia chromosome-positive acute lymphoblastic leukemia emerge after therapy with BCR-ABL kinase inhibitors. *Cancer.* 2008;113(5):985-994.
38. Skaggs BJ, Gorre ME, Ryvkin A, et al. Phosphorylation of the ATP-binding loop directs oncogenicity of drug-resistant BCR-ABL mutants. *Proc Natl Acad Sci U S A.* 2006;103(51):19466-19471.
39. Griswold IJ, MacPartin M, Bumm T, et al. Kinase domain mutants of Bcr-Abl exhibit altered transformation potency, kinase activity, and substrate utilization, irrespective of sensitivity to imatinib. *Mol Cell Biol.* 2006;26(16):6082-6093.
40. Miething C, Feihl S, Mugler C, et al. The Bcr-Abl mutations T315I and Y253H do not confer a growth advantage in the absence of imatinib. *Leukemia.* 2006;20(4):650-657.
41. Takayama N, Sato N, O'Brien SG, Ikeda Y, Okamoto S. Imatinib mesylate has limited activity against central nervous system involvement of Philadelphia chromosome-positive acute lymphoblastic leukemia due to poor penetration into cerebrospinal fluid. *Br J Hematol.* 2002;119(1):106-108.
42. Pfeifer H, Wassmann B, Hofmann WK, et al. Risk and prognosis of central nervous system leukemia in patients with Philadelphia chromosome-positive acute leukemias treated with imatinib mesylate. *Clin Cancer Res.* 2003;9(13):4674-4681.
43. Leis JF, Stepan DE, Curtin PT, et al. Central nervous system failure in patients with chronic myelogenous leukemia lymphoid blast crisis and Philadelphia chromosome positive acute lymphoblastic leukemia treated with imatinib (STI-571). *Leuk Lymphoma.* 2004;45(4):695-698.
44. Neville K, Parise RA, Thompson P, et al. Plasma and cerebrospinal fluid pharmacokinetics of imatinib after administration to nonhuman primates. *Clin Cancer Res.* 2004;10(7):2525-2529.

45. Porkka K, Koskenvesa P, Lundan T, et al. Dasatinib crosses the blood-brain barrier and is an efficient therapy for central nervous system Philadelphia chromosome-positive leukemia. *Blood.* 2008;112(4):1005-1012.

46. Lagas JS, van Waterschoot RA, van Tilburg VA, et al. Brain accumulation of dasatinib is restricted by P-glycoprotein (ABCB1) and breast cancer resistance protein (ABCG2) and can be enhanced by elacridar treatment. *Clin Cancer Res.* 2009;15(7):2344-2351.

47. Buonamici S, Trimarchi T, Ruocco MG, et al. CCR7 signaling as an essential regulator of CNS infiltration in T-cell leukemia. *Nature.* 2009; 459(7249):1000-1004.

48. Ottmann O, Dombret H, Martinelli G, et al. Dasatinib induces rapid hematologic and cytogenetic responses in adult patients with Philadelphia chromosome positive acute lymphoblastic leukemia with resistance or intolerance to imatinib: interim results of a phase 2 study. *Blood.* 2007; 110(7):2309-2315.

49. Balis FM, Lester CM, Chrousos GP, Heideman RL, Poplack DG. Differences in cerebrospinal fluid penetration of corticosteroids: possible relationship to the prevention of meningeal leukemia. *J Clin Oncol.* 1987;5(2):202-207.

50. Gómez-Almaguer D, Gonzalez-Llano O, Montemayor J, Jaime-Perez JC, Galindo C. Dexamethasone in the treatment of meningeal leukemia. *Am J Hematol.* 1995;49(4):353-354.

Table S1. Low frequency of BCR-ABL KD mutations after relatively brief dasatinib exposure

Experimental Group	**Mutational Frequency (% of mutant alleles)**			
	Bone Marrow	Spleen	Lymph nodes	Meninges
Vehicle (n=7)	0	0	0	0
Start of Rx (n=8)	0	0	0	0
Rx (1 week) (n=4)	0	20	0	0
Rx (2 weeks) (n=10)	15	4	0	0

Bone marrow, spleen, cervical lymph nodes, and meningeal tissue samples from the indicated cohorts of mice were analyzed for the presence of BCR-ABL KD mutations. Data represents the % of BCR-ABL alleles positive for a KD mutation. In all positive cases, the T315I mutation was detected.

Figure S1. Comparative potency of imatinib and dasatinib on cultured LICs. *Arf* $^{-/-}$; p185^{+} LICs were incubated with varying concentrations of dasatinib or imatinib (abscissa) for 72 hrs, and cell proliferation (ordinate) was quantified 72 hours later by use of a methane–thiosulfonate–based (MTS) assay (CellTiter 96 Aqueous One Solution assay reagent, Promega, Madison, WI). LICs established by short-term culture of transduced bone marrow progenitors [17,18] were maintained in RPMI 1640 medium (Bio-Whittaker, Lonza, Switzerland) supplemented with 10% fetal calf serum, 55 μM 2-mercaptoethanol, 2 mM glutamine, penicillin, and streptomycin. Cells were plated at 10^4 per well in 96-well plates. Dasatinib (LC Labs) stock solutions were prepared in DMSO (40 mM), and the drug was diluted in cell culture media to achieve the desired final concentrations; final DMSO concentrations were always ≤ 0.1%. Dasatinib IC_{50} was calculated to be 0.1 nM while that for imatinib was 100 nM, identifying dasatinib as 1000-fold more potent than imatinib in arresting cell growth.

Figure S2. BCR-ABL KD mutations arising after four weeks of dasatinib therapy. Cohorts of mice allowed to develop increasing initial leukemic cell burdens prior to treatment were started on dasatinib therapy 3, 7 or 10 days after LIC injection. Analysis of bone marrow (BM), spleen and cervical lymph node (LN) tissues from relapsed mice, the majority of which relapsed upon discontinuation of therapy, indicated that a longer duration of continuous dasatinib treatment is required for a significantly more frequent recovery of clones with KD mutations (see text Table 1, and Suppl. Fig. 3). ND = not determined.

Figure S3. BCR-ABL KD mutations are present at high frequencies in cohorts of mice relapsing after prolonged dasatinib treatment. The figure illustrates results of detailed analysis of KD mutations detected in hematopoietic tissues of relapsed mice that had received varying intensities of dasatinib therapy. A direct correlation between the frequency of the T315I mutation and intensity of dasatinib therapy was observed. P-loop mutations were not detected in mice that relapsed on the most intense treatment regimen. In three separate leukemic samples in which both T315I and P-loop mutations were detected in the same tissue, both mutations were not present on the same sequenced amplicon, suggesting that they arose as independent mutational events rather than sequentially during the course of therapy. See Suppl. Fig. 2 for color-coded figure key. ND = not determined

Figure S4. In vivo whole-animal luminescence reveals two phenotypes of disease distribution at relapse. Whole-animal luminescence revealed distributed sites of disease at the start of therapy (A) followed by significant reduction of disease after one week of therapy with residual pockets of resistant cells seen in the head and neck area (B). Disease distribution at relapse (C) was characterized either by disseminated infiltrates distributed throughout the whole body (top panel) or localized to the head area (bottom panel). Ventral and dorsal images are illustrated.

Figure S5. Leukemia infiltration at relapse from cohorts of mice receiving dexamethasone, L-asparaginase and/or dasatinib alone or in combination. Cohorts of mice received: vehicle alone (n=8), dasatinib alone (n=15), L-asparaginase alone (n=15), dexamethasone alone (n=16), L-asparaginase plus dexamethasone (n=15), dasatinib plus L-

asparaginase (n=14), dasatinib plus dexamethasone (n=10) and all three agents (n=4). Mice were analyzed for the presence of leukemia by determining their white blood cell (WBC) counts, spleen weights, or by quantifying *in vitro* luminescence signals in erythrocyte-free blood and bone marrow samples.

Fig S1

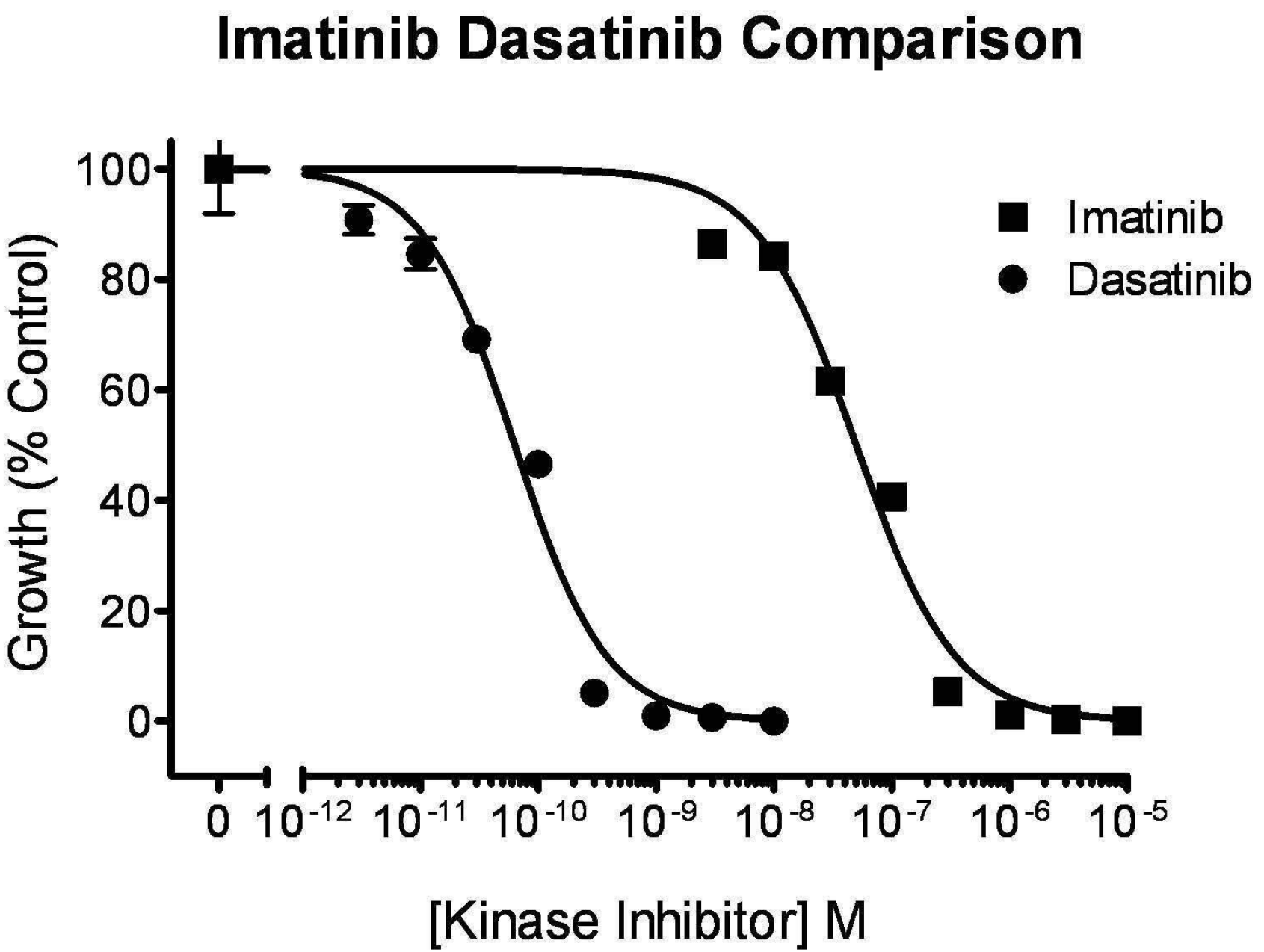
Imatinib Dasatinib Comparison
Growth (% Control)
100
80
60
40
20
0
Imatinib
Dasatinib
0
10-12
10-11
10-10
10-9
10-8
10-7
10-6
10-5
[Kinase Inhibitor] M

Fig S2

Treatment Group	Survival (Days)	Mutation Frequency		
		BM	Spleen	LN
Day 10	46			
	48			
	48			
	47			
	53			
	63			
	59			
	47			
	62			
	62			
	48			
	49			
Day 7	88			
	70			
	33			ND
	49			
	63			
Day 3	39			ND
Vehicle	13			ND
	13			ND
	13			ND
	13			ND

Mutation	Code	Frequency (%)
T315I		80-100
		50-79
		20-49
P-Loop		80-100
		50-79
		20-49
Absent		<20

Fig S3

Treatment Group	Survival (days)	Mutation Frequency		
		BM	Spleen	LN
Vehicle	13			ND
	13			ND
	13			ND
	13			ND
b.i.d 7 days/week	85			ND
	76			ND
	84			ND
	63			ND
	94			
	80			
	49			ND
	78			ND
b.i.d 5 days/week	67			ND
	59			ND
	59			ND
	59			ND
	38			ND
	42			
	27			
	38			
	38			
	63			
	37			
	38			
	31			ND
	31			ND
	49			
	60			ND
	49			
	52			
	38			
	38			
	38			
q.d 7 days/week	33			ND
	58			
	60			
	42			
	55			
	58			
	36			
	53			
q.d 5 days/week	38			ND
	32			ND
	38			
	53			
	38			ND
	38			

Fig S4

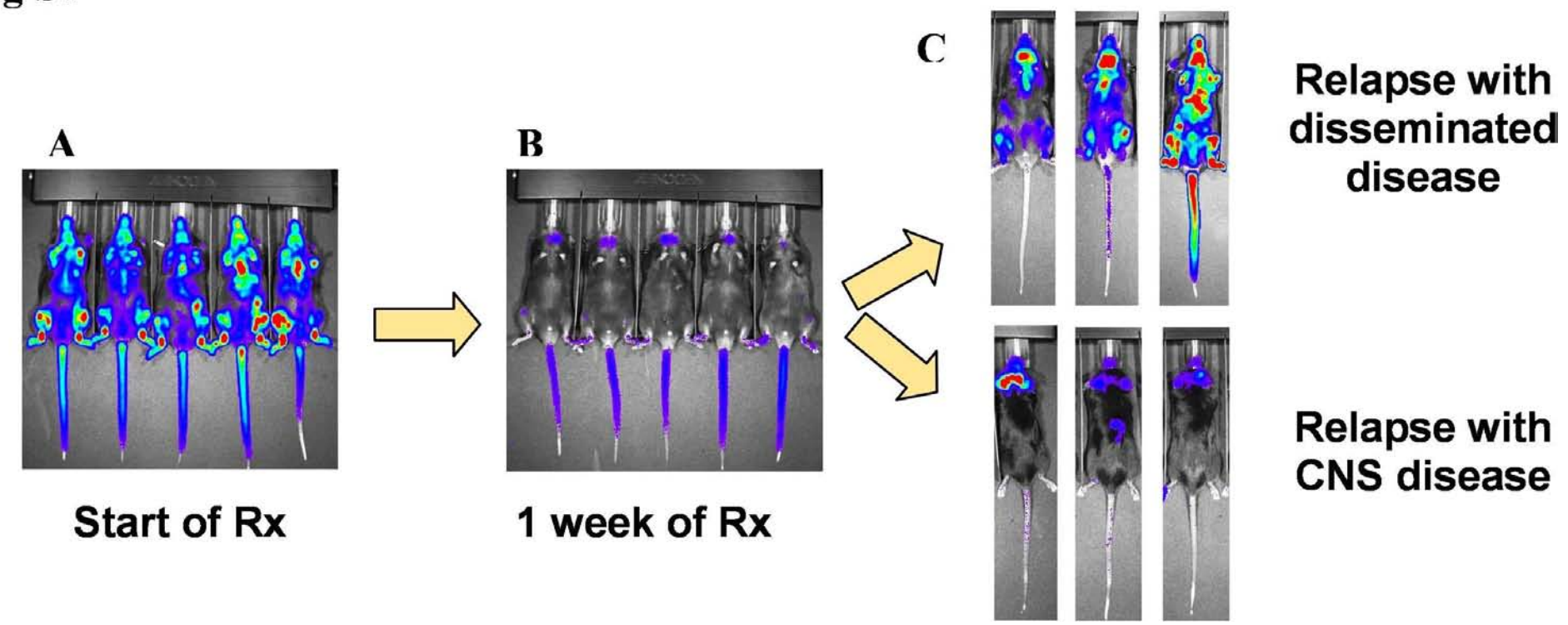
A
B
C
Start of Rx
1 week of Rx
Relapse with disseminated disease
Relapse with CNS disease

Fig S5

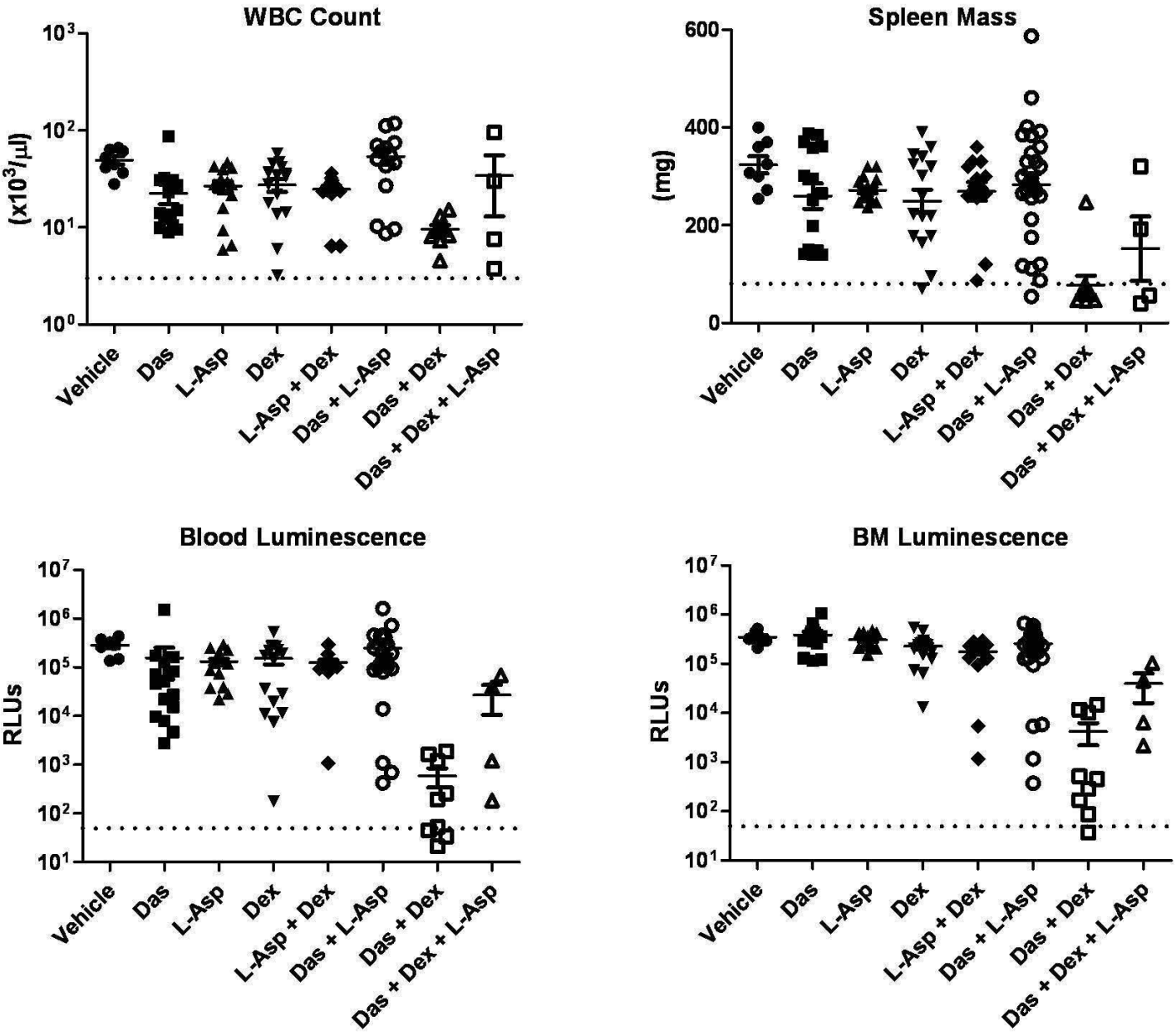
WBC Count
(x10^3/μl)
Spleen Mass
(mg)
Blood Luminescence
RLUs
BM Luminescence
RLUs
Vehicle
Das
L-Asp
Dex
L-Asp + Dex
Das + L-Asp
Das + Dex
Das + Dex + L-Asp